Available online at www.sciencedirect.com
SCIENCE DIRECT
Polymer 46 (2005) 11451–11462
polymer
www.elsevier.com/locate/polymer

Bulk free radical polymerizations of methyl methacrylate under non-isothermal conditions and with intermediate addition of initiator: Experiments and modeling

Jitendra S. Sangwai [a], Shrikant A. Bhat [a], Sanjay Gupta [b], Deoki N. Saraf [a,1], Santosh K. Gupta [a,*]

[a] Department of Chemical Engineering, Indian Institute of Technology, Kanpur, 208016, India
[b] Advanced Center for Materials Science, Indian Institute of Technology, Kanpur, 208016, India

Received 5 July 2005; received in revised form 27 September 2005; accepted 12 October 2005

Abstract

Experimental data on the monomer conversion, x_m, and the weight average molecular weight, M_w, have been generated under several isothermal and non-isothermal conditions for the polymerization of methyl methacrylate in a rheometer-reactor assembly. The non-isothermal results, in particular, can be used to provide more stringent tests of kinetic models than isothermal data alone. A simple empirical model has been used to describe this system that accounts for the gel (Trommsdorff) and glass effects. The model involves only x_m and the temperature, and is quite general. The model parameters are tuned using only three sets of isothermal data. Good agreement is found between the experimental results and model predictions for a whole variety of experimental conditions, including non-isothermal operation and with intermediate addition of initiator. Because of its generality, this model is quite suitable for use for on-line optimizing control as well as for describing industrial reactors.

Keywords: Bulk free radical polymerization; Kinetics; Non-isothermal polymerizations

1. Introduction

Modeling of bulk free radical polymerizations has always posed a challenge because of the complex nature of the diffusional processes associated with the reactions. These processes get accentuated with the increase in viscosities of the reaction mass with the progress of polymerization. The reaction scheme that describes several such systems is given in Table 1. The diffusional limitations are manifested in terms of the gel (Trommsdorff [1,2]), glass, and cage effects associated with the decrease in the diffusivities of the macro-radicals, monomer molecules and primary radicals, respectively. Considerable effort has been made to model these effects using empirical as well as fundamental approaches. Hui and Hamielec [3] and Ross and Laurence [4] correlated two of the apparent rate constants in Table 1, viz., those for chain propagation, k_p, and chain termination, k_t, in terms of the monomer conversion, x_m, and the temperature, T. Several other empirical models [5–9] were later developed to fit isothermal experimental data with different degrees of success. The latter models as well as that of Ross and Laurence correlated the rate constants with different parameters of the system like x_m, the weight average molecular weight, M_w, the free volume, etc., and involved break points characterizing the onset of diffusional limitations. Chiu et al. [10] proposed a model involving a fundamental molecular basis in which diffusional limitations affected the rate constants right from the beginning of polymerization. Their model accounted for the influence of T, x_m and M_w on the relative importance of reaction vs diffusion. This model had the advantage that it did not involve any discontinuities. Achilias and Kiparissides [11,12] proposed an improved model based on the generalized free volume theory of Vrentas and Duda [13–15] and the theory of excess chain-end mobility (Soh and Sundberg [16,17]). This theory involved the use of parameters that could be obtained from independent experiments on the physical and transport properties of the corresponding non-reacting monomer-polymer system. However, neither of these theories could be applied satisfactorily to polymerizations under non-isothermal conditions, or in cases with intermediate addition of compounds

* Corresponding author. Tel.: +91 512 259 7031/7127; fax +91 512 259 0104.
E-mail address: skgupta@iitk.ac.in (S.K. Gupta).
[1] Presently at University of Petroleum and Energy Studies, Dehradun, 248007, India.

0032-3861/$ - see front matter © 2005 Published by Elsevier Ltd.
doi:10.1016/j.polymer.2005.10.064

Nomenclature

$A_{i,1}$, $A_{i,2}$ empirical parameters ($i=1$–4) (K^{-1}, –)
$B_{i,1}$, $B_{i,2}$ empirical parameters ($i=1$–4) (K^{-1}, –)
C_m, C_R concentration of monomer and free radical (mol/m^3)
D diffusivity of the monomer in the monomer polymer mixture
D_n dead polymer molecule having n repeat units
f initiator efficiency in the limiting case of zero diffusional resistance
I initiator
$[I]_0$ concentration of initiator at $t=0$ ($mol\ m^{-3}$)
k_d rate constant for initiation in presence of the gel and glass effects (s^{-1})
k_p, k_t, k_{tm} rate constants for propagation, termination and chain transfer to monomer in presence of the gel and glass effects ($m^3\ mol^{-1}\ s^{-1}$)
k_{tc}, k_{td} rate constants for termination by combination and by disproportionation in the presence of the gel effect ($m^3\ mol^{-1}\ s^{-1}$)
k_{td}^0, k_p^0, k_{tm}^0 k_{td}, k_p, k_{tm} in absence of the gel or glass effects ($m^3\ mol^{-1}\ s^{-1}$)
k_{tdo}, k_{po}^0, k_{tmo}^0 frequency factors for the intrinsic rate constants (s^{-1} or $m^3\ mol^{-1}\ s^{-1}$)
l_{chr} length of chromosome
l_{str} length of substring
M monomer; moles of monomer in the liquid phase (mol)
M_w weight average molecular weight [$\equiv(MW_m)(\lambda_2+\mu_2)/(\lambda_1+\mu_1)$] ($kg\ kmol^{-1}$)
MW_m molecular weight of the monomer ($kg\ kmol^{-1}$)
n number of parameters in SGA
N_p population size
P_c probability of crossover
P_m probability of mutation
P_n growing polymer radical having n repeat units
r_m radius of reaction sphere
R primary radical
R_{li}, R_{lm} rate of continuous addition of initiator and monomer ($mol\ s^{-1}$)
R_{vm} rate of evaporation of monomer ($mol\ s^{-1}$)
$T(t)$ temperature of the reaction mixture at time t (K or °C)
t time (min)
V_l volume of liquid at time t (m^3)
$x_m(t)$ monomer conversion (molar) at time t [$\equiv 1-(M/\zeta_{m1})$]

Greek letters

α fraction of monomer molecule undergoing chain transfer
$\dot{\gamma}$ shear rate (s^{-1})
ζ_m, ζ_{m1} net monomer added to the reactor as defined by Seth and Gupta [19]
η viscosity of the reaction mass (Pa s)
λ_k k^{th} ($k=0$, 1, 2…) moment of live (P_n) polymer radicals $\left[\equiv\sum_{n=1}^{\infty} n^k P_n\right]$ (mol)
μ_k k^{th} ($k=0$, 1, 2…) moment of dead (D_n) polymer chains $\left[\equiv\sum_{n=1}^{\infty} n^k D_n\right]$ (mol)
μ_n number average chain length at time t [$\equiv(\lambda_1+\mu_1)/(\lambda_0+\mu_0)$]
ρ_m, ρ_p density of pure (liquid) monomer and polymer at temperature T ($kg\ m^{-3}$)
τ shear stress (Pa)
ϕ_m, ϕ_p volume fractions of monomer and polymer in liquid at time t

Subscripts superscripts

add addition
b bulk concentration
opt optimal value

(the latter is known as semi-batch operation), commonly encountered in industry. Ray et al. [18] and Seth and Gupta [19] extended these fundamental models semi-empirically and presented a new model to describe such systems. However, the predictions of this model were very sensitive to the values of the parameters involved, and this model did not work satisfactorily for on-line optimizing control applications [20]. Recently, a three stage model was proposed by Qin et al. [21,22], which employs a simple approach to model bulk free radical polymerizations under isothermal conditions. However, it is not possible to evaluate the boundaries of the three stages for any temperature history a priori, and this limits its usefulness. In addition, this approach cannot be extended to non-isothermal conditions, thus, limiting its application for industrial systems. A parallel and important development in the last decade has been the use of the pulsed laser polymerization (PLP) technique to determine the values of k_p and k_t for free radical polymerizations [23]. Barner-Kawollik et al. [24] have recently presented an extensive review of the experimental methods used to study the dependence of k_t on the conversion and chain length. Buback et al. [25] used this technique to obtain the chain length dependence of k_t for MMA polymerization. These experimental techniques can be used

Table 1
Kinetic scheme for the bulk free radical polymerizations

Initiation	$I \xrightarrow{fk_d} 2R$
Propagation	$R + M \xrightarrow{k_i} P_1$
	$P_n + M \xrightarrow{k_p} P_{n+1}$
Termination by combination	$P_n + P_m \xrightarrow{k_{tc}} D_{n+m}$
Termination by disproportionation	$P_n + P_m \xrightarrow{k_{td}} D_n + D_m$
Chain transfer to monomer	$P_n + M \xrightarrow{k_{tm}} P_1 + D_n$

Table 2
Mass balance and moment equations for bulk free radical polymerizations in semi-batch reactors [18]

$dI/dt = -k_d I + R_{li}(t)$
$dM/dt = -(k_p + k_{tm})(\lambda_0 M/V_l) + R_{lm}(t) - R_{vm}(t) - k_i(RM/V_l)$
$dR/dt = 2fk_d I - k_i(RM/V_l)$
$d\lambda_0/dt = k_i(RM/V_l) - k_t(\lambda_0^2/V_l)$
$d\lambda_1/dt = k_i(RM/V_l) + k_p M(\lambda_0/V_l) - k_t(\lambda_0\lambda_1/V_l) + k_{tm}M((\lambda_0 - \lambda_1)/V_l)$
$d\lambda_2/dt = k_i(RM/V_l) + k_p M((\lambda_0 + 2\lambda_1)/V_l) - k_t(\lambda_0\lambda_2/V_l) + k_{tm}M((\lambda_0 - \lambda_2)/V_l)$
$d\mu_0/dt = k_{tm}M(\lambda_0/V_l) + (k_{fd} + (1/2)k_{tc})(\lambda_0^2/V_l)$
$d\mu_1/dt = k_{tm}M(\lambda_1/V_l) + k_t(\lambda_0\lambda_1/V_l)$
$d\mu_2/dt = k_{tm}M(\lambda_2/V_l) + k_t(\lambda_0\lambda_2/V_l) + k_{tc}(\lambda_1^2/V_l)$
$d\zeta_m/dt = R_{lm}(t) - R_{vm}(t)$
$d\zeta_{m1}/dt = R_{lm}(t)$
$V_l = ((M(MW_m))/\rho_m) + ((\zeta_m - M)(MW_m))/\rho_p)$
$\phi_m = (M(MW_m)/\rho_m)/((M(MW_m)/\rho_m) + ((\zeta_m - M)(MW_m)/\rho_p))$
$\phi_p = 1 - \phi_m$
$k_d = k_{d,o}\exp(-E_d/RT)$
$k_p^0 = k_{p,o}^0\exp(-E_p/RT)$
$k_{fd}^0 = k_{fd,o}^0\exp(-E_{fd}/RT)$
$k_t = k_t^0\exp(A_1 + A_2x_m + A_3x_m^2 + A_4x_m^3)$; for $x_m > 0$
$k_p = k_p^0\exp(B_1 + B_2x_m + B_3x_m^2 + B_4x_m^3)$; for $x_m > 0$
$A_i = A_{i1}(T - 273.15) + A_{i2}$; $i = 1, 2, \ldots, 4$
$B_i = B_{i1}(T - 273.15) + B_{i2}$; $i = 1, 2, \ldots, 4$
Initial conditions
At $t = 0$
$I = I_0$; $M = \zeta_m = \zeta_{m1} = M_0$; $\lambda_0 = \lambda_1 = \lambda_2 = \mu_0 = \mu_1 = \mu_2 = R = 0$
Continuity conditions (for single addition of monomer and initiator at $t = t_1$)
$I(t_1^+) = I(t_1^-) + I_{add}$; $M(t_1^+) = M(t_1^-) + M_{add}$; $\zeta_m(t_1^+) = \zeta_m(t_1^-) + M_{add}$; $\zeta_{m1}(t_1^+) = \zeta_{m1}(t_1^-) + M_{add}$

to develop even more detailed models for k_t and k_p in the near future, that can explain polymerizations under a variety of conditions.

Although the use of molecular approaches for modeling the rates of polymerization did lead to fundamental insights, the more successful models have been the empirical ones. A detailed comparison of these models was done by Tefera et al. [26,27]. Hui and Hamielec [3] presented this family of empirical models as early as in 1972, expressing $k_p/k_t^{1/2}$ in terms of x_m and T:

$$\frac{k_p}{k_t^{1/2}} = \left[\frac{k_p^0}{k_t^{0\,1/2}}\right]\exp\left(A_1x_m + A_2x_m^2 + A_3x_m^3\right) \quad (1)$$

In Eq. (1), $A_1 - A_3$ are empirical parameters and superscript, o, indicates values in the absence of the gel and glass effects. They expressed the parameters, $A_1 - A_3$, as linear functions of temperature ($A_i = \alpha_i + \beta_i T$), and obtained exact correlations for a few systems. Recently, Curteanu and Bulacovschi [28] extended Eq. (1) and related k_t and k_p, individually, to x_m as

$$k_t = k_t^0\exp\left(A_1 + A_2x_m + A_3x_m^2 + A_4x_m^3\right) \quad (2a)$$

$$k_p = k_p^0\exp\left(B_1 + B_2x_m + B_3x_m^2 + B_4x_m^3\right) \quad (2b)$$

These workers obtained individual sets of values for the model parameters, A_i and B_i, using experimental data [29] at different (isothermal) temperatures and initiator loadings, $[I]_0$, as well as for near-step changes in temperature [30] and for intermediate addition of initiator [31]. Unfortunately, they did not attempt to provide generalized correlations for these parameters, as was done by Hui and Hamielec [3], so that they could apply for all conditions. This limits the usefulness of Eq. (2). A major fundamental drawback of Eq. (2) is that it does not reduce to $k_p = k_p^o$ and $k_t = k_t^o$ at $x_m = 0$, nor can it be interpreted as involving two additional parameters, k_p^0 and k_t^o, to be tuned using experimental data. Hence, this equation is associated with some physical contradictions. As such, Eq. (2) should be looked at as a purely empirical model.

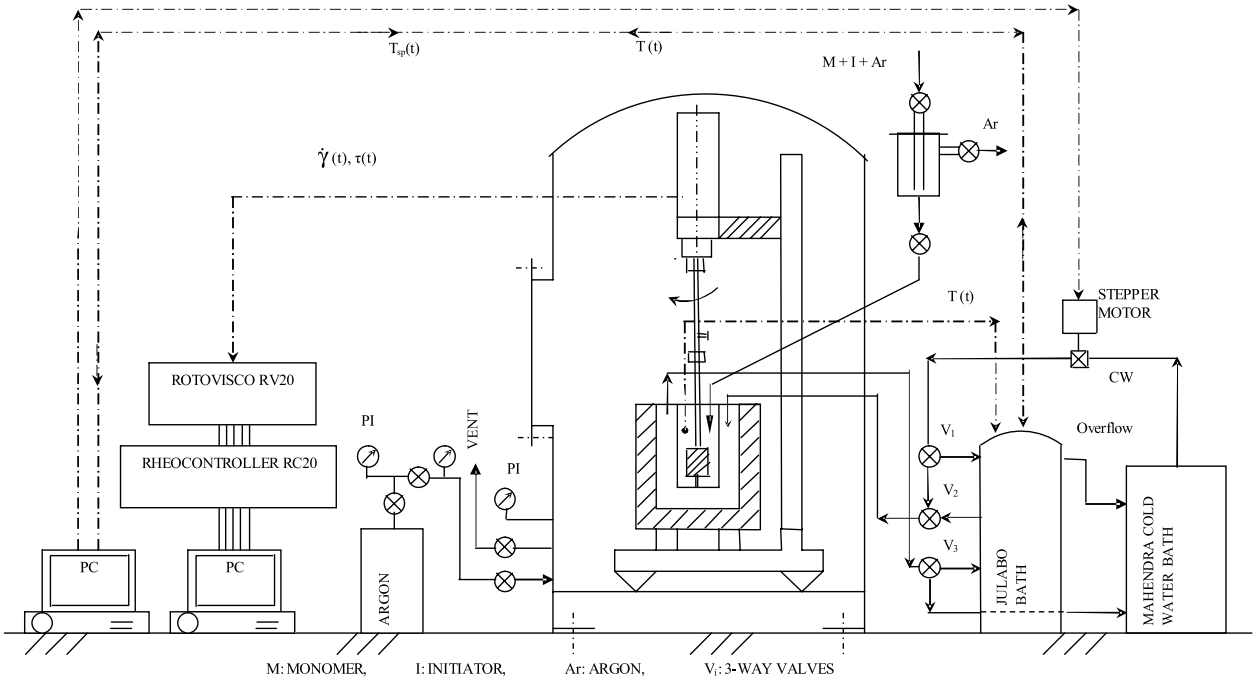

Fig. 1. Schematic diagram of the experimental set-up.

Table 3
Parameters used for solving the model equations [18]

ρ_m	$966.5-1.1(T-273.15)$ kg m^{-3}
ρ_p	1200 kg m^{-3}
f	0.58
k_d^0	1.053×10^{15} s^{-1}
$k_{p,o}^0$	4.917×10^{2} m^3 mol^{-1} s^{-1}
$k_{td,o}^0$	9.800×10^{4} m^3 mol^{-1} s^{-1}
k_{fm}^0	4.66×10^{6} m^3 mol^{-1} s^{-1}
k_{fc}	0.0
k_t	k_{td}
k_i	k_p
k_{fm}/k_{fm}^0	k_p/k_p^0
E_d	128.45 kJ mol^{-1}
E_p	18.22 kJ mol^{-1}
E_{td}	2.937 kJ mol^{-1}
(MW_m)	0.10013 kg mol^{-1}
(MW_I)	0.06800 kg mol^{-1}

In this study, Eq. (2) is generalized using the method of Hui and Hamielec [3]. A simple linear dependence of the eight parameters on the temperature is assumed. The parameters are then 'tuned' using only three sets of available data [29] on monomer conversion, under isothermal conditions. It is found that such a tuned model can predict almost all other experimental data extremely well. In addition to this, eleven new sets of experimental data are generated in this study under isothermal and non-isothermal [step increase (SI) and step decrease (SD) in temperature] conditions at values of $[I]_0$ of 15.48 and 25.8 mol/m^3. These have been taken in a rheometer-reactor assembly [32] in which there is excellent heat transfer, and the temperature is the same as the 'measured' values. The near-isothermal results obtained in this study superpose with earlier results [29] taken on small glass ampoules, and so confirm the conclusions of Zhu and Hamielec [33] that the data of Balke and Hamielec [29] are, indeed, trustworthy, and that the studies of Armitage et al. [34] and Gao and Penlidis [35] showed extensive amounts of non-isothermality because of low rates of heat transfer and high concentrations of the initiator. The additional new data reported, particularly under non-isothermal conditions, provides more stringent tests of models. Good agreement with model predictions is observed for a wide variety of experimental conditions. The correlation developed is, we believe, very general and can be used under almost any other experimental conditions, as well as under conditions used industrially [36].

Table 4
Computational parameters and bounds used in SGA

Computational parameters		
n	16	
N_p	50	
P_c	0.9	
P_m	0.003	
l_{chr}	240	
l_{str}	15	
Tuning parameter	Lower bound	Upper bound
Bounds		
A_{11}, K^{-1}	−0.04	−0.01
A_{12}	0.7	1.0
A_{21}, K^{-1}	−0.5	0
A_{22}	8	12
A_{31}, K^{-1}	0	0.2
A_{32}	−39	−32
A_{41}, K^{-1}	−0.002	−0.001
A_{42}	2	3.5
B_{11}, K^{-1}	−0.005	−0.004
B_{12}	0.1	0.2
B_{21}, K^{-1}	−0.4	−0.2
B_{22}	7.5	9.5
B_{31}, K^{-1}	0.099	0.3
B_{32}	8	10.5
B_{41}, K^{-1}	0.2	0.4
B_{42}	−50	−38

Table 5
Details of the near-isothermal (NI) experimental runs

No	Run No	$[I]_0$ (mol/m^3)	Experimental temp history[a] T(°C)
1	NI70	15.48	$47.911-3.6659t+2.2769t^2-0.1875t^3$; $t<7.95$; 70; $t\geq7.95$
2	NI70	25.80	$47.911-3.6659t+2.2769t^2-0.1875t^3$; $t<7.95$; 70; $t\geq7.95$
3	NI80	15.48	$45.886+0.4438t+0.9716t^2-0.0674t^3$; $t<8.52$; 80; $t\geq8.52$
4	NI80	25.80	$45.886+0.4438t+0.9716t^2-0.0674t^3$; $t<8.52$; 80; $t\geq8.52$

[a] t in min.

2. Kinetic model

The mass balance and moment equations [18,19], valid for general operating conditions, are given in Table 2. This table also incorporates Eqs. (2). Chain transfer to monomer is also incorporated in this study. This reaction is associated with a rate constant, k_{tm}. Since the molecular processes (bulk diffusion of monomer towards a growing macro-radical, followed by segmental diffusion and collision of the reactive end of the macro-radical with the monomer) involved in chain transfer are similar to those in propagation, a molecular model can easily be developed for k_{tm}. The concept of the reaction sphere, as proposed by Chiu et al. [10] is used. It is assumed that the monomer molecules in the reaction sphere are consumed both by propagation as well as by chain transfer (competing events). If the fraction of monomer molecules undergoing chain transfer is α, then the fraction of monomer

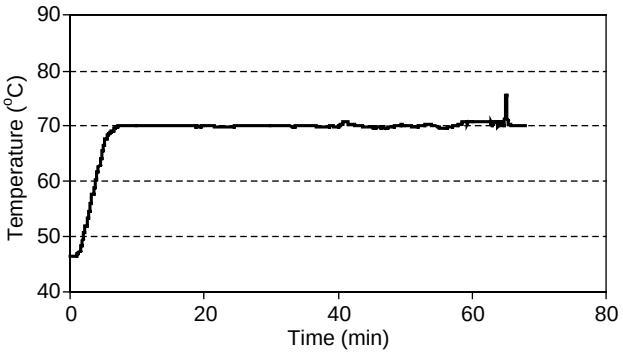

Fig. 2. Experimental temperature history for a near-isothermal run at 70 °C; $[I]_0=15.48$ mol/m^3.

molecules undergoing propagation would be $(1-\alpha)$. Since only the *intrinsic* rate constants are involved inside this reaction sphere of radius, r_m, we can write:

$$\alpha = \frac{k_{tm}^0 M\lambda_0}{k_{tm}^0 M\lambda_0 + k_p^0 M\lambda_0} = \frac{k_{tm}^0}{k_{tm}^0 + k_p^0} \tag{3}$$

where M and λ_o are values inside the reaction sphere. The development of Chiu et al. [10] can be used to give (see Nomenclature)

$$4\pi D r_m (C_{mb} - C_m) = \frac{4}{3}\pi r_m^3 \left[\alpha k_{tm}^0 + (1-\alpha)k_p^0\right] C_{Rb} C_m \equiv \frac{4}{3}\pi r_m^3 k^0 C_{Rb} C_m \tag{4}$$

This can be used with

$$k_{tm} C_{mb} C_{Rb} = k_{tm}^0 C_m C_{Rb} \tag{5}$$

to give

$$\frac{1}{k_{tm}} = \frac{1}{k_{tm}^0} + \frac{k^0 r_m^2 \lambda_0}{3 k_{tm}^0 D V_1} \tag{6}$$

The expression for k_p, in the presence of chain transfer, is obtained in a similar manner as

$$\frac{1}{k_p} = \frac{1}{k_p^0} + \frac{k^0 r_m^2 \lambda_0}{3 k_p^0 D V_1} \tag{7}$$

Eqs. (6) and (7) give

$$\frac{k_{tm}}{k_{tm}^0} = \frac{k_p}{k_p^0} \tag{8}$$

Eq. (8) has been used by several workers [37–39] earlier but had been written using intuitive arguments.

Table 3 gives the values of the parameters to be used while solving the equations in Table 2. The temperature dependence of the parameters, A_i ($i=1$ to 4) and B_i (i = 1 to 4), in Eq. (2) are assumed to be given by

$$A_i = A_{i1}(T - 273.15) + A_{i2}; \quad i = 1, 2, 3, 4 \tag{9a}$$

$$B_i = B_{i1}(T - 273.15) + B_{i2}; \quad i = 1, 2, 3, 4 \tag{9b}$$

The values of the sixteen empirical parameters in Eq. (9) are obtained (tuned) using only three sets of experimental data [29] on $x_m(t)$ [and not $M_w(t)$]: at 50 and 90 °C at $[I]_0 = 15.48$ mol/m^3, and at 70 °C at $[I]_0 = 25.8$ mol/m^3, all under isothermal conditions. A code for simple genetic algorithm, SGA [40], is used to carry out this exercise. The tuning is done by minimizing the normalized sum of square errors, E, between the experimental data on x_m and the model-predicted values

$$\text{Min } E(A_{i,1}, B_{i,1}, A_{i,2}, B_{i,2}; i = 1,2,3,4) = \sum_{i=1}^{n_x} \left[\left(\frac{x_{m,mod}(t_i) - x_{m,exp}(t_i)}{x_{m,mod}(t_i)} \right)^2 \right] \tag{10}$$

In Eq. (10), subscripts mod and exp represent the model-predicted and experimental values, respectively, and n_x is the total number of data points available for x_m. Table 4 gives the computational parameters used as well as the upper and lower bounds of the sixteen parameters.

3. Experimental set-up

Several experimental runs under near-isothermal and non-isothermal (near-step increase and decrease in temperature) conditions are carried out in a Haake® (M5 osc, Haake® Mess-Technik GmbH, Germany) viscometer modified to work as a viscometer-reactor assembly (for details, see Ref. [32]). The schematic diagram of the experimental set-up is shown in Fig. 1. The set-up is an adapted version of that used by Mankar et al. [32], and uses two constant temperature baths [Julabo® F10-MH (Julabo Labortechnik GmbH, Germany), Mahendra® (Mahendra Instruments, Kanpur, India)] instead of a single one used in our previous study. This helps to overcome the thermal inertia of the system and provides a rapid step decrease of temperature, which was not possible with a single bath. The Haake® (SV2) cup is modified so as to have a hollow chamber around the gap of the viscometer (see Fig. 1 in Ref. [20]). The desired temperature histories (isothermal as well as non-isothermal) are obtained by circulating water at appropriate temperatures through this chamber, using the three 3-way valves, $V_1 - V_3$, in Fig. 1. The Julabo® bath incorporates a PID controller with auto-tuning features. It is able to track desired near-isothermal temperature histories as well as cases involving near-step increases in the temperature. However, it is unable to provide rapid decreases in temperatures because of the large heat capacity of the cup-and-bob assembly. To achieve faster responses in such cases, cold water at about 20 °C from the Mahendra® bath is taken to the water storage tank of the Julabo® unit (at controlled flow rates using a stepper motor-actuated needle valve and the PID controller of the Julabo® bath). A Pt-100 temperature sensor is dipped inside the reaction mass just above the viscometer gap in the cup and bob assembly. This gives the temperature of the reaction mass. The rheometer-reactor assembly enables polymerization to be carried out in the annular gap between the cup and the bob under almost any desired temperature history. The rheometer-reactor assembly is placed in a pressure vessel with Argon at 150–350 kPa. This suppresses the formation of vapor bubbles inside the reaction mass.

The details of the purification procedure for the monomer, the initiator (2, 2′- azoisobutyronitrile, AIBN), and the experimental procedure for carrying out the polymerization in the rheometer-reactor assembly are given elsewhere [29,32] and are not repeated here. Several identical experiments are carried out and the reaction mass in the viscometer gap is quenched at different times by lowering its temperature by circulating water at about 5 °C from the Mahendra® unit. These samples are taken out from the viscometer gap and analyzed. x_m is obtained gravimetrically while M_w is determined using dilute solution viscometry using an Ubbelhode viscometer (No. 501 01, Schott-Gerate, Hofheim, Germany). The use of a thin (thickness = 1.45 mm) annular region for polymerization with the *metallic* bob rotating continuously ensures excellent heat transfer and mixing, and there are no temperature gradients in

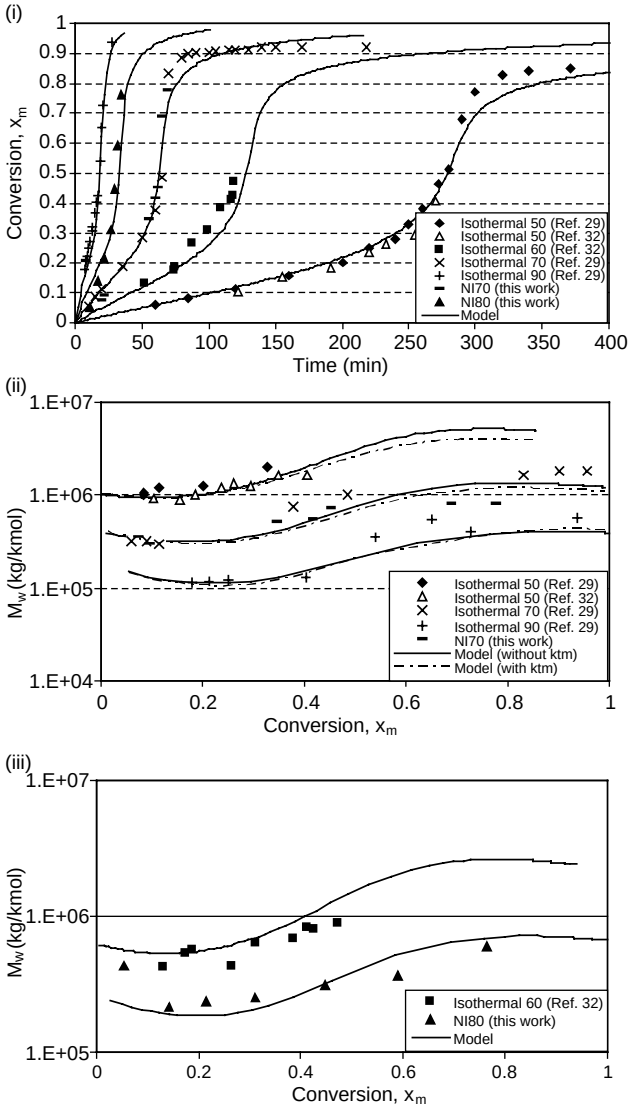

Fig. 3. Experimental data on x_m and M_w for isothermal and near isothermal conditions ($[I]_0 = 15.48$ mol/m^3). Solid curves show model predictions.

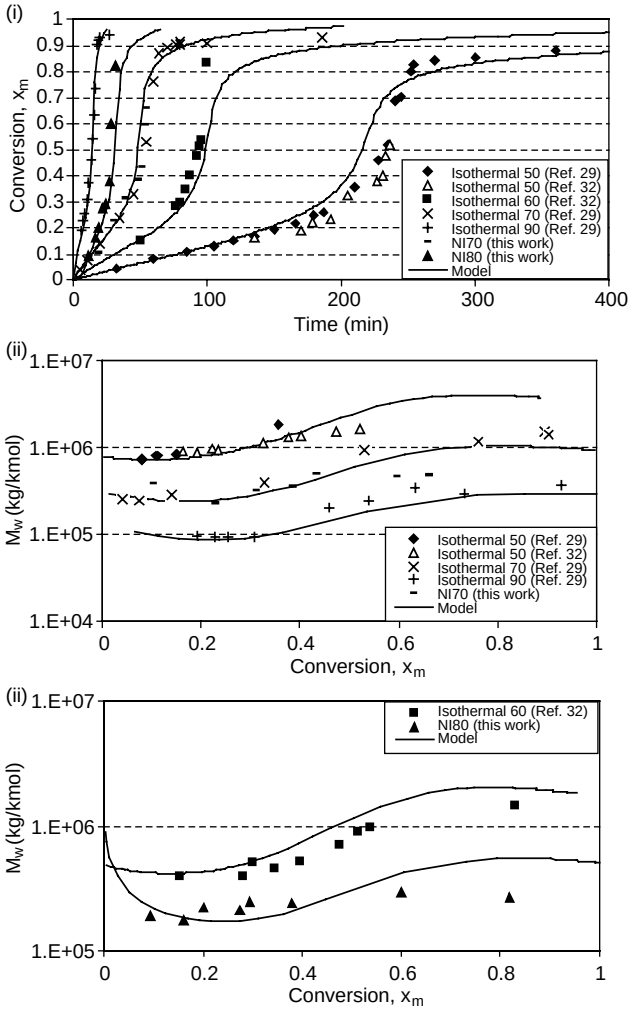

Fig. 4. Experimental data on x_m and M_w for isothermal and near isothermal conditions ($[I]_0 = 25.8$ mol/m^3). Solid curves show model predictions.

the reaction mass [20,32]. The data so taken are, therefore, expected to be quite trustworthy.

4. Results and discussion

4.1. Experimental

We present new experimental data generated in this study first, and then present our results on parameter estimation. Four near-isothermal (NI) runs have been carried out. The details are summarized in Table 5. Fig. 2 shows the experimental temperature history for one case. The temperature goes up from the initial value of about 45 °C (due to preheating of the cup) to the set-point of 70 °C. The control of the temperature is quite good, the temperature being controlled within ±0.5 °C most of the time. The exothermic heat generated at the onset of the gel effect is removed by circulating water at about 5 °C directly from the Mahendra® water bath through the hollow chamber in the cup for a very short period of time. Fig. 2 shows that the temperature is reasonably well controlled (at about 70 min) by this procedure. The data on $T(t)$ is fitted to an empirical equation for use in the model equations. The fitted equations for $T(t)$ for all the four experimental runs are given in Table 5. x_m and M_w are obtained at several values of t for all these cases. Our values of x_m and M_w at (near-isothermal)

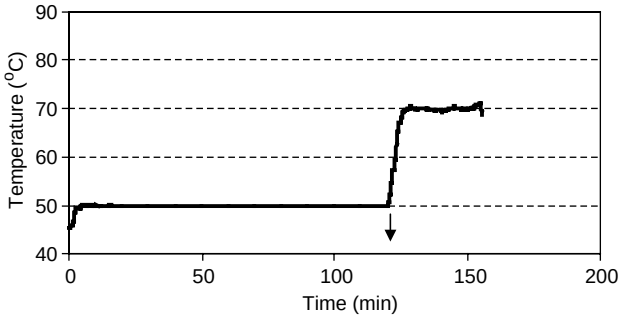

Fig. 5. Experimental temperature history for a near-step increase in temperature from 50 to 70 °C at 120 min [SI 50(120)70]; $[I]_0 = 15.48$ mol/m^3. The arrow indicates the time at which the set-point is changed.

Table 6
Details of the non-isothermal experimental runs

No	Run No	$[I]_0$ (mol/m^3)	Experimental temp history[a] T(°C)	Comment
1	SI50(120)70	15.48	50; $t<120$; $49.574+2.9406(t-120)+0.5098(t-120)^2-0.0733(t-120)^3$; $120\le t<127.63$; 70; $t\ge 127.63$	Step increase from 50 to 70 °C at 120 min
2	SI50(120)70	25.8	50; $t<120$; $49.574+2.9406(t-120)+0.5098(t-120)^2-0.0733(t-120)^3$; $120\le t<127.63$; 70; $t\ge 127.63$	Step increase from 50 to 70 °C at 120 min
3	SI50(60)70	15.48	50; $t<60$; $49.58+1.8019(t-60)+0.5768(t-60)^2-0.0613(t-60)^3$; $60\le t<68.4$; 70; $t\ge 68.4$	Step increase from 50 to 70 °C at 60 min
4	SI50(60)70	25.8	50; $t<60$; $49.58+1.8019(t-60)+0.5768(t-60)^2-0.0613(t-60)^3$; $60\le t<68.4$; 70; $t\ge 68.4$	Step increase from 50 to 70 °C at 60 min
5	SI50(100)60	25.8	50; $t<60$; $49.815+1.036(t-100)+0.8965(t-100)^2-0.1442(t-100)^3$; $100\le t<104.0$; 60; $t\ge 104.0$	Step increase from 50 to 60 °C at 100 min
6	SD70(20)50	15.48	$46.825-0.7373t+1.5014t^2-0.133t^3$; $t<7.85$; 70; $7.85\le t<20$; $70.557-2.8423(t-20)-1.3506(t-20)^2+0.3662(t-20)^3-0.0247(t-20)^4$; $20\le t<27.55$; 50; $t\ge 27.55$	Step decrease from 70 to 50 °C at 20 min
7	SD70(20)50	25.8	$46.825-0.7373t+1.5014t^2-0.133t^3$; $t<7.85$; 70; $7.85\le t<20$; $70.557-2.8423(t-20)-1.3506(t-20)^2+0.3662(t-20)^3-0.0247(t-20)^4$; $20\le t<27.55$; 50; $t\ge 27.55$	Step decrease from 70 to 50 °C at 20 min

[a] t in min.

70 °C for $[I]_0=15.48$ mol/m^3 as well as 25.8 mol/m^3 are plotted in Figs. 3 and 4. Our data are found to superpose extremely well with those of Balke and Hamielec [29] [see plots for NI70 (this work) and Isothermal 70 (Ref. [29]) in Figs. 3 and 4]. This gives confidence on our experimental techniques. The superposition of our data (wherein the possibility of non-isothermality is small) with those taken in small glass ampoules [29] for both values of $[I]_0$, further confirms [33] that the data of Balke and Hamielec [29] are trustworthy. Our data are found to extend to well within the gel effect region (the viscometer used in this work slips above some high value of the torque). The data (for two values of $[I]_0$) at near-isothermal 80 °C and shown in Figs. 3 and 4, are new and help in the development of a good tuned model.

Fig. 5 shows the experimental temperature history for a run involving a (near) step increase in the temperature from 50 to 70 °C at 120 min [Run SI50(120)70]. The step change in the temperature is achieved within 6–7 min. Several similar non-isothermal experimental runs were carried out. Table 6 gives the curve-fitted temperature histories and other details for five such cases involving a step increase in temperature. Figs. 6–8 give the experimental results for x_m(t) and M_w(t) for all these cases. The five sets of data, namely, SI50(120)70 and SI50(60)70 at $[I]_0=15.48$ and 25.8 mol/m^3, and SI50(100)60 at $[I]_0=25.8$ mol/m^3, for step increases in temperature, are new. Such data, under non-isothermal (and semi-batch) conditions, are required for developing models that can be applied to industrial systems, and, in fact, provide stringent tests of models for the kinetics of polymerizations. Only one SI run (SI1 in Fig. 7 and Table 7) has been reported earlier [30] at $[I]_0=25.8$ mol/m^3 and our data under similar temperature histories superposes reasonably well with these (see Fig. 7), but extends to much higher values of x_m.

Figs. 9 and 10 show the experimental results for $x_m(t)$ and $M_w(t)$ for two cases involving a (near) step decrease in

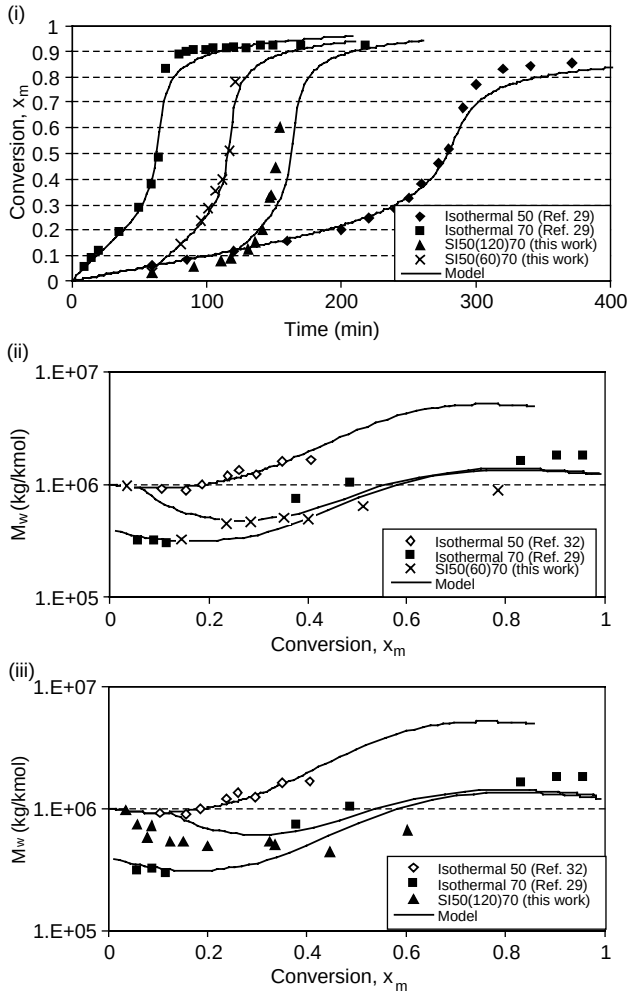

Fig. 6. Experimental data on x_m and M_w for runs involving near-step increase in temperature ($[I]_0=15.48$ mol/m^3). Solid curves show model predictions.

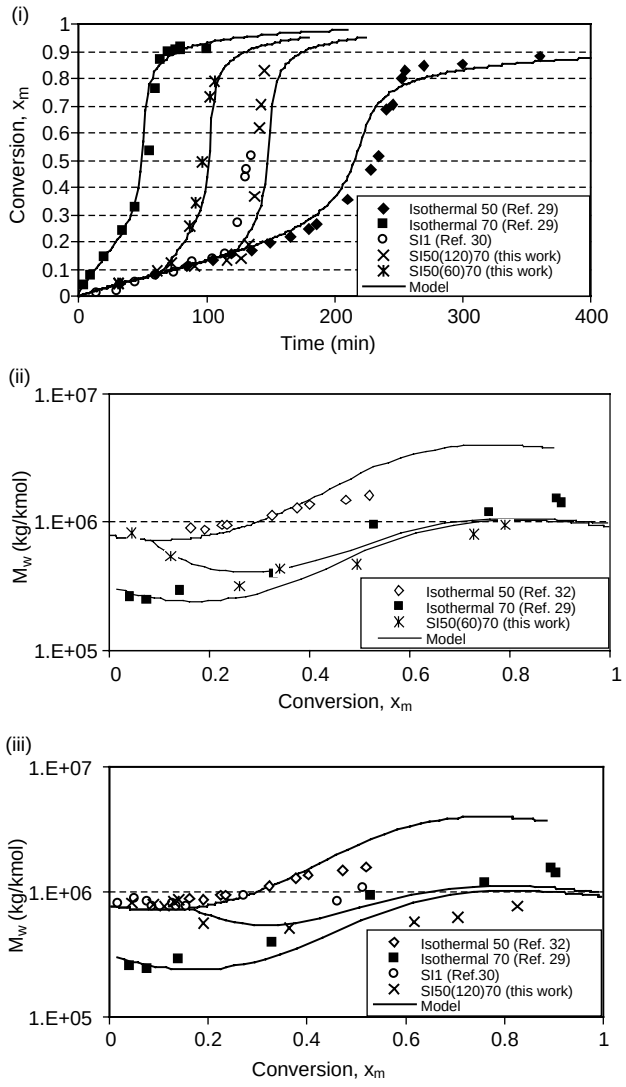

Fig. 7. Experimental data on x_m and M_w for runs involving near-step increase in temperature ($[I]_0 = 25.8$ mol/m^3). Solid curves show model predictions. Table 7 gives details of the SI1 run.

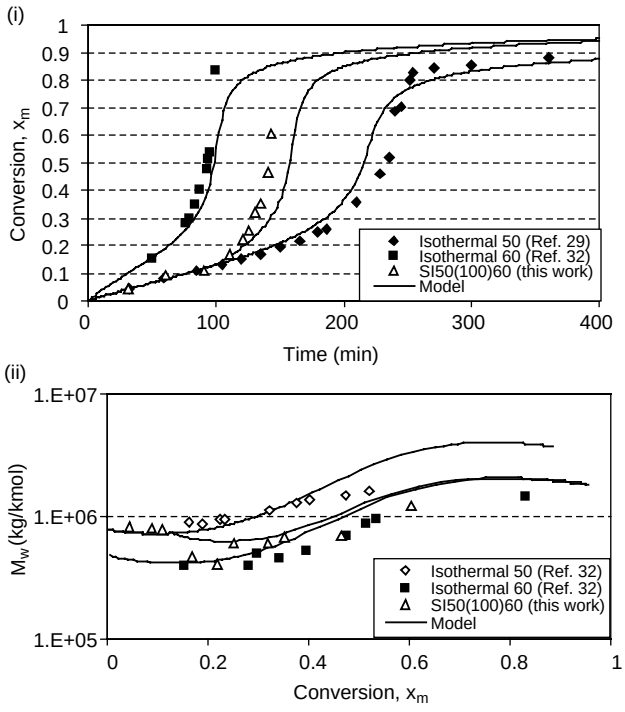

Fig. 8. Experimental data on x_m and M_w for step increase in temperature condition ($[I]_0 = 25.8$ mol/m^3). Solid curves show model predictions.

temperature [SD70(20)50 at $[I]_0 = 15.48$ and 25.8 mol/m^3]. This data is also new. Fig. 10 shows two more sets of near-step decrease data (SD1 and SD2) available in the literature [30], the details of which are summarized in Table 7. Our SD70(20)50 results on $x_m(t)$ are found to lie in-between the isothermal results [29] at 70 and 50 °C, as expected. In contrast, the $x_m(t)$ results of Srinivas et al. [30] under almost the same conditions [SD1 or SD70(25)50] are found to go even beyond the isothermal results at 50 °C after some value of t. Later, we find that our tuned model (which is found to agree with data for a whole variety of other experimental conditions, both isothermal and non-isothermal) agrees with our experimental data for the SD70(20)50 run. Curteanu and Bulacovschi [28] also had to re-tune their model parameters for this particular case because their original model gave entirely different predictions. It seems that our previous data [30] for near-step decrease of temperature, and taken in a 1-liter batch reactor, may be having errors. It may be added here that data (not reported here) on viscosity vs time taken for over ten SD70(20)50 runs (before being quenched), did superpose extremely well over common ranges of t, indicating that our present data are trustworthy. As opposed to this, reproducibility was not checked as extensively in our earlier study [30] since several samples could easily be withdrawn at different times from the reactor in a single experiment itself.

4.2. Model-tuning

Only three sets of isothermal data [29] [$T = 50$ and 90 °C at $[I]_0 = 15.48$ mol/m^3; $T = 70$ °C at $[I]_0 = 25.8$ mol/m^3] on $x_m(t)$ are used to tune the model parameters in Eq. (9a,9b).

Table 7
Experimental runs carried out by Srinivas et al. [30] and Dua et al. [31]

No	Run No	$[I]_0$; mol/m^3	$T(t)$
1	SI1 [30]	25.8	SI50(120)70
2	SD1 [30]	25.8	SD70(25)50
3	SD2 [30]	25.8	SI70(45)50
4[a]	IA50(170) [31]	15.48	Initiator addition at 170 min, at $T = 50$ °C
5[a]	IA50(90) [31]	15.48	Initiator addition at 90 min, at $T = 50$ °C
6[a]	IA70(28) [31]	15.48	Initiator addition at 28 min, at $T = 70$ °C

[a] A solution of 75 ml of monomer having an initiator concentration of 550.7 mol/m^3 is added to 400 ml of the (initial) batch, at the desired time. Temperatures are near-isothermal in these cases.

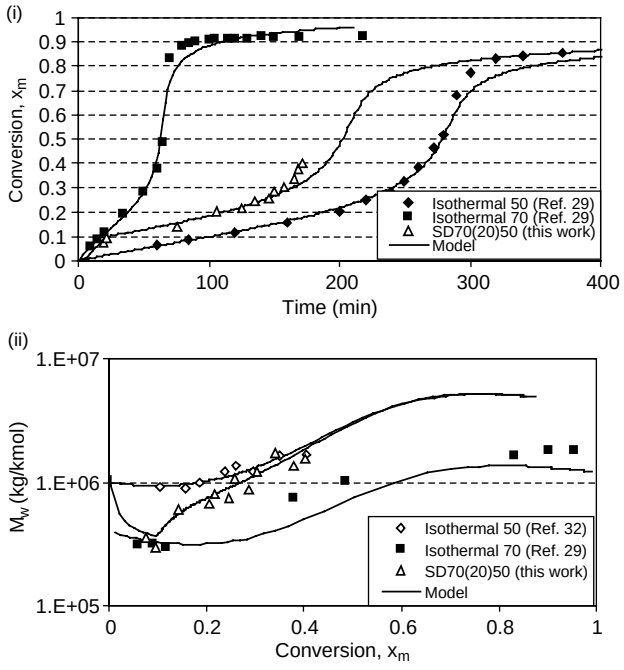

Fig. 9. Experimental data on x_m and M_w for step decrease in temperature condition ($[I]_0 = 15.48$ mol/m^3). Solid curves show model predictions. The model plots for this work differ slightly from those in Ref. [29] because of the small differences in the initial temperature histories.

The tuning has been carried out both with and without chain transfer. The two sets of values of the parameters are given in Table 8. We also tried to tune these parameters using three sets of experimental data [29] under the same conditions as before on both $x_m(t)$ and $M_w(t)$. Unfortunately, this worsened the model predictions, possibly because of the scatter in the data on $M_w(t)$. Hence, the data on $M_w(t)$ was not included for tuning.

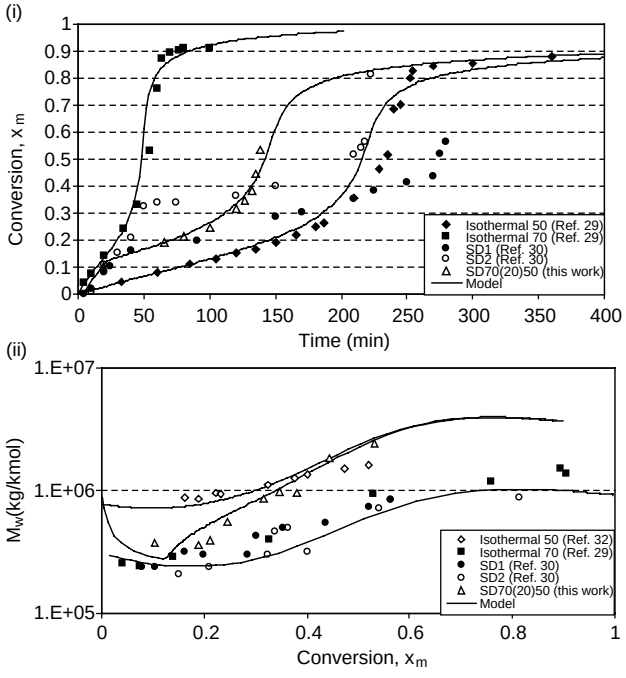

Fig. 10. Experimental data on x_m and M_w for step decrease in temperature condition ($[I]_0 = 25.8$ mol/m^3). Solid curves show model predictions.

Table 8
Tuned values of the parameters in Eq. (9)

	A_{11} (K^{-1})	A_{12}	A_{21} (K^{-1})	A_{22}	A_{31} (K^{-1})	A_{32}	A_{41} (K^{-1})	A_{42}	B_{11} (K^{-1})	B_{12}	B_{21} (K^{-1})	B_{22}	B_{31} (K^{-1})	B_{32}	B_{41} (K^{-1})	B_{42}
With-out k_m	-2.242×10^{-2}	8.151×10^{-1}	-2.531×10^{-1}	9.425	1.213×10^{-1}	-3.656×10^{1}	-1.234×10^{-3}	3.404	-4.886×10^{-3}	1.211×10^{-1}	-2.782×10^{-1}	9.464	1.641×10^{-1}	8.619	2.767×10^{-1}	-4.098×10^{1}
With k_m	-2.293×10^{-2}	7.973×10^{-1}	-2.379×10^{-1}	8.784	1.385×10^{-1}	-3.609×10^{1}	-1.745×10^{-3}	2.223	-4.020×10^{-3}	1.246×10^{-1}	-3.054×10^{-1}	9.734	2.706×10^{-1}	8.278	2.493×10^{-1}	-4.459×10^{1}

Table 9
The correlation matrix and confidence intervals for the parameters (without k_{tm}) in Table 8

S	A_{11}	A_{12}	A_{21}	A_{22}	A_{31}	A_{32}	A_{41}	A_{42}	B_{11}	B_{12}	B_{21}	B_{22}	B_{31}	B_{32}	B_{41}	B_{42}
Correlation matrix																
A_{11}	1	−0.467	0.156	−0.512	−0.127	−0.153	−0.178	−0.255	0.210	0.354	0.065	−0.352	0.290	−0.234	0.070	−0.403
A_{12}		1	0.019	0.136	0.352	0.171	−0.094	0.090	−0.196	−0.093	0.287	0.228	−0.321	0.102	−0.308	0.134
A_{21}			1	−0.787	0.257	−0.284	−0.121	−0.125	0.338	0.321	0.867	−0.075	−0.249	−0.092	−0.129	−0.041
A_{22}				1	−0.326	0.148	0.354	0.347	−0.414	−0.545	−0.660	0.183	0.160	0.166	−0.041	0.152
A_{31}					1	0.207	−0.579	−0.092	0.448	0.037	0.437	0.204	−0.501	0.165	0.009	0.281
A_{32}						1	−0.119	−0.076	0.046	−0.028	−0.065	−0.173	−0.033	0.342	0.138	0.101
A_{41}							1	0.247	−0.491	−0.282	−0.227	0.144	0.151	−0.165	−0.107	−0.132
A_{42}								1	−0.122	−0.390	−0.084	0.292	0.021	−0.190	−0.336	0.051
B_{11}									1	0.422	0.263	0.079	−0.318	0.326	0.211	0.112
B_{12}										1	0.288	−0.346	−0.120	0.096	0.149	−0.138
B_{21}											1	−0.195	−0.330	−0.066	−0.304	−0.057
B_{22}												1	−0.523	0.018	0.002	0.154
B_{31}													1	−0.366	−0.244	−0.076
B_{32}														1	0.522	−0.011
B_{41}															1	−0.044
B_{42}																1

Sr. No	Parameter	Lower limit	Upper limit	Mean values (Table 9)
Confidence intervals (95%)				
1	A_{11}, K^{-1}	-2.628×10^{-2}	-1.855×10^{-2}	-2.242×10^{-2}
2	A_{12}	6.856×10^{-1}	9.445×10^{-1}	8.151×10^{-1}
3	A_{21}, K^{-1}	-3.322×10^{-1}	-1.739×10^{-1}	-2.531×10^{-1}
4	A_{22}	7.735	1.112×10^{1}	9.425
5	A_{31}, K^{-1}	1.982×10^{-2}	2.229×10^{-1}	1.213×10^{-1}
6	A_{32}	-3.765×10^{1}	-3.546×10^{1}	-3.656×10^{1}
7	A_{41}, K^{-1}	-1.840×10^{-3}	-6.274×10^{-4}	-1.234×10^{-3}
8	A_{42}	2.642	4.167	3.404
9	B_{11}, K^{-1}	-5.429×10^{-3}	-4.343×10^{-3}	-4.886×10^{-3}
10	B_{12}	5.690×10^{-2}	1.853×10^{-1}	1.211×10^{-1}
11	B_{21}, K^{-1}	-3.178×10^{-1}	-2.385×10^{-1}	-2.782×10^{-1}
12	B_{22}	8.531	1.040×10^{1}	9.464
13	B_{31}, K^{-1}	1.128×10^{-1}	2.154×10^{-1}	1.641×10^{-1}
14	B_{32}	7.191	1.005×10^{1}	8.619
15	B_{41}, K^{-1}	1.952×10^{-1}	3.583×10^{-1}	2.767×10^{-1}
16	B_{42}	-4.251×10^{1}	-3.945×10^{1}	-4.098×10^{1}

The model predictions for $x_m(t)$ and $M_w(t)$ incorporating chain transfer are not very different from those without this mechanism, as shown in Fig. 3(ii) for three cases (Isothermal 50, 70 and 90 °C, at $[I]_0 = 15.48$ mol/m^3). The model predictions for $x_m(t)$ are almost identical for the two tuned models, and are not shown in Fig. 3(i). Because of this, chain transfer is not considered henceforth. The correlation matrix and confidence intervals for the parameters obtained (without considering k_{tm}) are given in Table 9. Since the model involves coupled ordinary differential equations, conventional approaches cannot be applied to perform statistical analysis. Hence, the bootstrap method [41] is used to achieve this. The detailed procedure for the evaluation of the correlation matrix and the confidence intervals of the parameters is given in Appendix A.

Figs. 3 and 4 compare the experimental results with the model predictions for the three cases used for tuning. The agreement is quite good both for $x_m(t)$, used for tuning, as well as for $M_w(t)$, which was not used to fit the model parameters. In fact, it is much better than the agreement obtained earlier [19] when the simplified model (BFCs: Best-Fit Correlations) of Seth and Gupta [19] was used to fit isothermal data [29]. The model predictions are also compared with experimental results for several near-isothermal experimental runs in Figs. 3 and 4. Excellent agreement is obtained for all cases studied (including data of Mankar et al. [32] at NI60), not only for $x_m(t)$, but also for $M_w(t)$. The use of only a small set of experimental data for tuning followed by excellent predictions of the tuned model for several other experimental runs, suggests that the model is excellent. Moreover, the model predictions do not change too much (as for the previous model [19]) with changes in the model parameters in the present case.

The applicability of such a tuned model to industrial systems and to on-line optimizing control, where non-isothermal temperature histories are present, is now tested. The predictions of the tuned model for several non-isothermal cases are shown in Figs. 6–10. Again, good agreement is observed between experimental results and model predictions for all the experimental SI runs. For the step decrease (SD) runs, however, we obtain interesting results. Fig. 9 shows good agreement for the SD70(20)50 runs of the present study for both $[I]_o = 15.48$ and 25.8 mol/m^3. However, our experimental

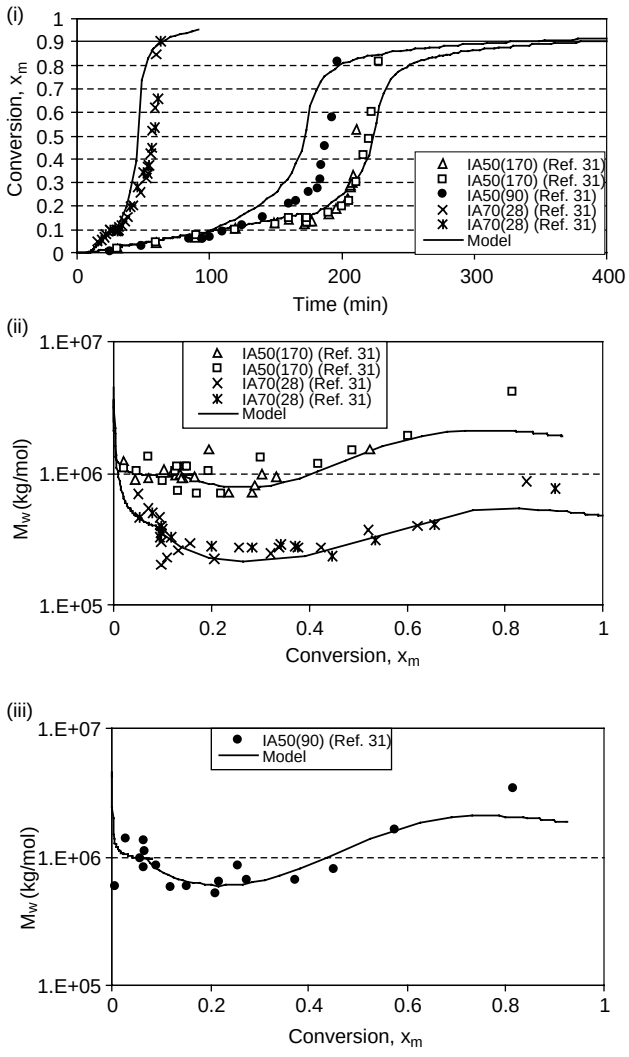

Fig. 11. Experimental data on x_m and M_w for initiator addition of Dua et al. [31]. Solid curves show model predictions.

results for $[I]_o = 25.8$ mol/m^3 differ qualitatively from those of Srinivas et al. [30] under similar conditions [their SD1 is SD70(25)50, while their SD2 is SD70(45)50]. We believe that the latter results involve some error. This is further confirmed by the fact that Curteanu and Bulacovschi [28] had to re-tune their model parameters for this set of data of Srinivas et al., because their original model gave entirely different predictions.

Fig. 11 shows the predictions of the present model for our earlier [31] experimental results involving intermediate addition (IA) of a solution of monomer and initiator. These experiments are carried out under near-isothermal conditions of 50 and 70 °C. The details of these runs are summarized in Table 7. The agreement between model predictions and experimental results for both $x_m(t)$ and $M_w(t)$ is not so good, although it is far better than observed with the model of Seth and Gupta [19]. The poor agreement, however, cannot be attributed to any fundamental aspects at this stage, looking at the empirical nature of the correlations for k_t and k_p. This, however, does not limit the use of the model since the model predictions are reasonably good for most of the other experimental conditions. It must also be emphasized that the predictions for these 'not so good' runs using the generalized empirical parameters do give some reasonable trend (although with a shift), which can be improved using on-line tuning of the parameters. This is a routine practice as far as the use of such empirical correlations is concerned in the industry.

The empirical model of Ross and Laurence [4] relates $\ln(k_p/k_p^o)$ and $\ln(k_t/k_t^o)$ to the temperature and the fractional free volume, V_f. The latter depends on the volume fraction of the monomer, which, in turn, is related to x_m. Their model involves discontinuities at two different values of V_f, 0.05 (for k_p) and 0.152 (for k_t). They fit six sets of isothermal data [29] on MMA polymerization, and find that their model is quite reasonable. The present model can be shown to be an extension of this model, involving higher order terms in x_m. This helps avoid discontinuities. In addition, the model has been tested against considerable amount of non-isothermal data and data with intermediate addition of initiator, to establish its generality. Indeed, the lack of a 'good' kinetic model was a major stumbling block for the development of soft sensors [32] for PMMA reactors, and led to poor on-line optimizing control [20] in our previous study.

5. Conclusion

The empirical model suggested in this study has several advantages over the models previously available in the literature. The important aspects are its simplicity, and the use of the same set of parameters for all cases, isothermal, non-isothermal, as well as conditions involving the intermediate addition of initiator. This model, therefore, is better suited for on-line state estimation and on-line optimizing control applications. In addition to this model, this study presents eleven new sets of experimental results on x_m and M_w under near-isothermal and non-isothermal conditions at different initiator loadings, data which provide excellent tests for the correlation developed.

Acknowledgements

Financial support from the Department of Science and Technology, Government of India, New Delhi [through grant III-5(13)/2001-ET] is gratefully acknowledged. Acknowledgement is also due to Professor D. Kundu of the Department of Mathematics, IIT, Kanpur, for help with the statistical analysis of data, Mr. J.S. Virdi for fabricating the viscometer-reactor assembly, and Mr. D.D. Pal for help regarding instrumentation.

Appendix A. Details of the Bootstrap Method [41] used to calculate the Correlation Matrix

A.1. Preliminary information:

The following three sets of data are used to tune the sixteen parameters of the kinetic model:

Conversion at 50 °C, $I_0 = 15.48$ mol/m^3 (18 points)
Conversion at 70 °C, $I_0 = 25.8$ mol/m^3 (14 points)
Conversion at 90 °C, $I_0 = 15.48$ mol/m^3 (15 points) (Total = 47 points)

A.2. The bootstrap method:

We arbitrarily select 10 points from each of the above cases (thus selecting a total of 30 data points for each trial), and evaluate (tune) the sixteen parameters of the kinetic model for this trial set. For each of the above cases, we retain the end points [i.e. the value of the first (initial time) and the last (final time) experimental data (monomer conversion)], and arbitrarily select other eight points from the remaining data. Four such random sets (different sets of 10 points) are generated for each of the cases (1, 2 and 3 above). This leads to a total of $4 \times 4 \times 4 = 64$ trial sets. This gives 64 sets of values of the tuned kinetic parameters. The mean values of the kinetic parameters are taken as those obtained by tuning with respect to the *entire* set of 47 data points, as given in Table 8. Using the 64 different sets of kinetic parameters and their mean values, we calculate the variance and covariance for each pair, thus forming a 16×16 correlation matrix, using MATLAB (see Table 9).

References

[1] Trommsdorff VE, Köhle H, Lagally P. Makromol Chem 1947;1:169–98.
[2] Norrish RGW, Smith RR. Nature 1942;150:336–7.
[3] Hui AW, Hamielec AE. J Appl Polym Sci 1972;16:749–69.
[4] Ross RT, Laurence RL. In: Bouton TC, Chappelear DC, editors. Continuous polymerization reactors, No. 160. AIChE Symp Ser, New York, 1976;72:74-79.
[5] Cardenas JN, O'Driscoll KF. J Polym Sci Polym Chem Edn 1976;14: 883–97.
[6] Arai K, Saito SJ. Chem Eng Jpn 1976;9:302–13.
[7] Schmidt AD, Ray WH. Chem Eng Sci 1981;36:1401–10.
[8] Marten FL, Hamielec AE. In: Henderson HN, Bouton TC, editors. Polymerization reactors and processes, Vol. 104. Washington, DC: ACS Symp Ser; 1979. p. 43–69.
[9] Tulig TJ, Tirrel M. Macromolecules 1981;14:1501–11.
[10] Chiu WY, Carratt GM, Soong DS. Macromolecules 1983;16:348–57.
[11] Achilias DS, Kiparissides C. J Appl Polym Sci 1988;35:1303–23.
[12] Achilias DS, Kiparissides C. Macromolecules 1992;25:3739–50.
[13] Vrentas JS, Duda JL. J Polym Sci Polym Phys Edn 1977;15:403–16.
[14] Vrentas JS, Duda JL. J Polym Sci Polym Phys Edn 1977;15:417–39.
[15] Vrentas JS, Duda JL. AIChE J 1979;25:1–24.
[16] Soh SK, Sundberg DC. J Polym Sci Polym Chem Edn 1982;20:1315–29.
[17] Soh SK, Sundberg DC. J Polym Sci Polym Chem Edn 1982;20:1331–44.
[18] Ray AB, Saraf DN, Gupta SK. Polym Eng Sci 1995;35:1290–9.
[19] Seth V, Gupta SK. J Polym Eng 1995;15:283–326.
[20] Mankar RB, Saraf DN, Gupta SK. J Appl Polym Sci 2002;85:2350–60.
[21] Qin J, Guo W, Zhang Z. Polymer 2002;43:1163–70.
[22] Qin J, Guo W, Zhang Z. Polymer 2002;43:4859–67.
[23] Beuermann S, Buback M, Davis TP, Gilbert RG, Hutchinson RA, Olaj OF, et al. Macromol Chem Phys 1997;198:1545–60.
[24] Barner-Kowollik C, Buback M, Egorov M, Fukuda T, Goto A, Olaj OF, et al. Prog Polym Sci 2005;30:605–43.
[25] Buback M, Egorov M, Feldermann A. Macromolecules 2004;37: 1768–76.
[26] Tefera N, Weickert G, Westerterp KR. J Appl Polym Sci 1997;63: 1649–61.
[27] Tefera N, Weickert G, Westerterp KR. J Appl Polym Sci 1997;63: 1663–80.
[28] Curteanu S, Bulacovschi V. J Appl Polym Sci 1999;74:2561–70.
[29] Balke ST, Hamielec AE. J Appl Polym Sci 1973;17:905–49.
[30] Srinivas T, Sivakumar S, Gupta SK, Saraf DN. Polym Eng Sci 1996;36: 311–21.
[31] Dua V, Saraf DN, Gupta SK. J Appl Polym Sci 1996;59:749–58.
[32] Mankar RB, Saraf DN, Gupta SK. Ind Eng Chem Res 1998;37:2436–45.
[33] Zhu S, Hamielec AE. Polymer 1991;32:3021–5.
[34] Armitage PD, Hill S, Johnson SF, Mytytiuk J, Turner JMC. Polymer 1988;29:2221–8.
[35] Gao J, Penlidis A. J Macromol Sci, Rev Macromol Chem Phys 1996;C36: 199–404.
[36] Zhou F, Gupta SK, Ray AK. J Appl Polym Sci 2001;81:1951–71.
[37] Vaid NR, Gupta SK. Polym Eng Sci 1991;31:1708–18.
[38] Kapoor B, Gupta SK, Varma A. Polym Eng Sci 1989;29:1246–58.
[39] Curteanu S, Bulacovschi V. Chem Ind 2004;58:393–400.
[40] Goldberg DE. Genetic Algorithms in Search, Optimization and machine learning, Addison-Wesley: Reading, MA, 1989.
[41] Efron B, Tibshirani RJ. An Introduction to the bootstrap. NY: Chapman and Hall; 1993.